Effects of UVA disappearance and presence on the acylated anthocyanins formation in grape berries

Haining Yin [a], Lin Wang [a], Fucheng Wang [b], Zhumei Xi [a],[*]

[a] *College of Enology, Northwest A&F University, Yangling, Shannxi Province, People's Republic of China*
[b] *Penglai Vine and Wine Technology Research Extension Center, Penglai, Shandong Province, People's Republic of China*

ARTICLE INFO

ABSTRACT

Ultraviolet A (UVA), the major component of the UV, plays a crucial role in formatting the characteristics of color in wine grapes by influencing its anthocyanin composition and contents. Results showed that anthocyanin biosynthesis was suppressed by UVA screening and enhanced by irradiation. The acetylation and *p*-coumaroylation of anthocyanins were more pronounced and showed positive correlation with a* and negative correlation with L*, b*, C*, and h, thereby leading to changes in color. Weighted gene co-expression network analysis showed that two modules (red and turquoise) were significantly related to the acetylation and p-coumaroylation of peonidin. In addition, relative gene expression assays and correlation analysis also indicated that *VvMYBA1* might influence anthocyanin accumulation by directly regulating *VvOMT* expression and increasing the flux to the vacuole through *VvGST4*. In conclusion, the results helped in improving our understanding of the role of UVA in skin color formation.

1. Introduction

Owing to the commercial importance of wine grapes (*Vitis vinifera* L.), it is vitally important to understand the effects of environmental factors on skin coloration as this knowledge may contribute to ensuring a more stable production of high-quality grapes (Blancquaert, Oberholster, Ricardo-da-Silva, & Deloire, 2019; Figueiredo-Gonzalez, Cancho-Grande, & Simal-Gandara, 2013). Due to the recent changes in the climate, the intensity and proportion of different spectral components have garnered progressively more attention in terms of their role in color formation(Cheng, Wei, & Wu, 2015; Zhang et al., 2021). Among these components, ultraviolet (UV) radiation is essential for the induction of specific phenolic compounds in grapes, such as flavonoid, flavonol, anthocyanin, and stilbenoid (Del-Castillo-Alonso et al., 2021; Fernandes de Oliveira & Nieddu, 2016a). Anthocyanins are red pigments that appear during veraison and remain till the end of harvesting, eventually contributing to the formation and composition of skin color (de Oliveira, Mercenaro, Del Caro, Pretti, & Nieddu, 2015; Fernandes de Oliveira & Nieddu, 2016a). Meanwhile, the accumulation and partitioning of anthocyanins in berry skin are determined by UV components (Fernandes de Oliveira & Nieddu, 2016a).UV radiation comprises of UVA (315 to 400 nm), UVB (280 to 315 nm), and UVC (<280 nm) (Blancquaert,

Oberholster, Ricardo-da-Silva, & Deloire, 2019; Kolb et al., 2001; Pfuendel, 2003). UVA and UVB are the only components that can reach the Earth's surface and affect plant physiology in the field. UVA, owing to its abundance, plays a considerable role in formatting secondary metabolites. These findings indicated the role of the UVA spectra components in the regulation of anthocyanin biosynthesis in berry skins of wine grapes.

Previously, studies have reported that grape berry skin pigments were mainly anthocyanins, including 3-*O*-monoglucosides and 3,5-*O*-diglucosides of Cyanidin (Cy), Peonidin (Pn), Malvidin (Mv), Petunidin (Pt), and Delphinidin (Dp) (He et al., 2010; Zhang et al., 2018). Flavonoid synthesis can be initiated through the phenylpropanoid pathway to produce coumaroyl-CoA (Luo et al., 2021). Coumaroyl-CoA subsequently transforms into dihydroflavonols and flavonols, which are catalyzed by chalcone synthase (CHS), chalcone isomerase (CHI), flavanone 3-hydroxylase (F3H), flavonoid 3′-hydroxylase (F3′H), flavonoid 3′5′-hydroxylase (F3′5′H), and flavonol synthase (FLS) (Azuma, Yakushiji, Koshita, & Kobayashi, 2012; Bogs, Jaffé, Takos, Walker, & Robinson, 2007; Luo et al., 2021). The second phase is critical for yellow coloration owing to the accumulation of chalcones, flavones, and flavonols (Luo et al., 2021). Furthermore, the third phase involves the synthesis of a series of stable anthocyanins catalyzed by

---

dihydroflavonol 4-reductase (DFR), leucoanthocyanidin dioxygenase (LDOX), UDP-glucose flavonoid 3-O-glucosyl-transferase (UFGT), O-methyltransferase (OMT), anthocyanin acyltransferase (AAT), and glutathione S-transferase (GST) (Bogs, Jaffé, Takos, Walker, & Robinson, 2007; Zhang et al., 2018). These structural genes on the anthocyanin pathway are also controlled by transcriptional regulation. Recently, different transcription factors (TFs) were reported to regulate the following structural genes on specific branches of the pathway involved in anthocyanin biosynthesis: *VvMYBPA1*, *VvMYBA1*, *VvMYBA3* (Bogs, Jaffé, Takos, Walker, & Robinson, 2007; He et al., 2010; Zhang et al., 2018). Furthermore, the ratio of tri- to di-hydroxylated and methylated to non-methylated anthocyanins are determined by the MYB TFs (Azuma, 2018).

In recent years, reports on UV radiation have primarily been related to their function and application on leaves (Pfuendel, 2003; Pfuendel, Ben Ghozlen, Meyer, & Cerovic, 2007; Zhang et al., 2012). Total anti-oxidant capacities of leaf extracts were positively correlated with the intensity of solar UV (Csepregi, Teszlak, Korosi, & Hideg, 2019). UVB irradiation could be a primary factor for UV inhibition of photosynthesis by attenuating the maximum photochemical yield of photosystem II (psII), this suggested that psII is protected against UVB damage by epidermal screening (Kolb et al., 2001; Pfuendel, 2003). Consequently, wavelength-dependent absorption may alter the spectral quality and quantity after light passes through the leaf. In our previous study, we observed that the ratio of UVA was higher in the bunch zone than in the canopy (data has not been published). Furthermore, compared with flesh and seeds, skin is the most UV-responsive part of a grape (Del-Castillo-Alonso et al., 2021). Therefore, the lack of a pink and uniform coloration on berry skins is frequently observed when the bunch zone is fully shaded. UVB and UVC irradiation reportedly did not affect the number of anthocyanins in grapes (Cantos, Espín, Fernández, Oliva, & Tomás-Barberán, 2003; Cantos, García-Viguera, de Pascual-Teresa, & Tomás-Barberán, 2000). The absence of UVA light may be responsible for a poor color, suggesting that skins have adapted photoreceptors to UVA. UV irradiation can stimulate the expression of the genes involved in anthocyanin biosynthesis and thereby enhance anthocyanin accumulation in numerous plants (Pfuendel, Ben Ghozlen, Meyer, & Cerovic, 2007; Zhang et al., 2012). In a case study, increasing UVA exposure intensity enhanced anthocyanin accumulation in Gros Colman grapes; furthermore, promoters of the grape DFR and LDOX genes could be induced via the UVA/blue receptor signal transduction pathway (Gollop, Even, Colova-Tsolova, & Perl, 2002; Gollop, Farhi, & Perl, 2001; Kataoka, Sugiyama, & Beppu, 2003). However, studies on reporting candidate genes for anthocyanin biosynthesis in UVA radiation are limited.

Until now, only a few studies have examined the relationship between UVA irradiation and anthocyanin biosynthesis in grape berries. We studied the effects of UVA radiation on anthocyanin biosynthesis in 'Cabernet Sauvignon' grape berries under field conditions and in vitro culture. Grape berries were subjected to UVA irradiation and used for transcription and metabolism analysis. Differently expressed genes (DEGs) and metabolic profiles were identified and characterized. Candidate genes responsible for UVA were further investigated. The molecular mechanisms of UVA that regulated anthocyanin levels were discussed. In the present study, we aimed to elucidate the effects of UVA light quality on the biosynthesis of flavonoids, specifically anthocyanins, in the skin of wine grapes during veraison.

2. Materials and methods

2.1. Vineyard conditions and field treatments

The experiment was conducted in a Northwest A&F University demonstration vineyard of 'Cabernet Sauvignon' wine grape (*Vitis vinifera* L.) in Yangling, Shannxi Province, China (N 34°18′9″, E 108°05′12″). The vineyard was maintained through a spur pruning system per year during two consecutive seasons, 2020 and 2021. The vines were trained on an overhead trellis system covered with a trans-lucent plastic film (1.0 × 70 m). In both seasons, vines were cane-pruned with 7–8 buds per cane. Grape clusters from 24 vines were divided into six groups with four vines (replicates) in each group, and grape clusters were covered with transparent UVA screening (UVA−) light filter film (NLK-UV99, NANOLINK, Shanghai, China) and no-screening (CK) light filter film (Base film, NANOLINK, Shanghai, China) bags composed of strips of a 25-μm thick polyethylene terephthalate (PET) film for 30 days after flowering (Figure S1). The PET film detailed data and average temperature during bagging is provided in Table S1. The temperatures within the bags of the UVA− and CK groups were approximate values; thus, we compared the intergroup effects of solar UVA without consid-ering the temperature. Grape clusters were sampled at 40, 54, 68, 82, 96, 103 DAT (days after treatment) from each treatment with eight bio-logical replicates. A total of 96 grape clusters were collected per vintage, including 48 grape clusters from the UVA- treatment and the others from CK treatment. The berries of the clusters were separated and immedi-ately frozen in liquid nitrogen and stored at −40 °C for the subsequent experimentation.

2.2. Intact detached grape clusters in vitro culture and UVA light treatments

Grape clusters of uniform size and color (green), that did not show any defects or mechanical damage were selected (a total of 18 clusters). Clusters with 2 % sucrose solution were placed in an incubator (RXZ-1000C, Ningbo Jiangnan Instrument Factory, China), and a constant temperature (25℃ ± 1℃) and humidity (80 %). Nine clusters were irradiated with UVA light (UVA+), and nine clusters were not exposed to light (Dark). Dark treatment clusters were bagged in three-layered paper bags (yellow-black-black). Grape clusters were irradiated from the top (100 cm) with a UVA 340 lamp equipped with four lamps of 20 W each (UVA340, Longpro, China). Irradiation was performed as per the con-dition mentioned in Table S2 at 1.1 W/m² fluency in the UVA light channel (with a maximum wavelength of 340 nm, Fig. S2a) to obtain the best overlap with ambient spectra (Fig. S2b). Samples were collected at 3, 6, and 9 DAT. At each sampling time, three clusters were randomly collected from UVA+ and Dark treatment, respectively. The skin of the berries was separated and immediately frozen in liquid nitrogen and stored at −80℃ for the subsequent experimentation.

2.3. Measurement of essential berry quality

A total of 50 grape berries were randomly collected from UVA- and CK treatment, respectively. The seeds were removed, and the flesh was homogenized manually at room temperature. Total soluble solids, fructose, glucose, titratable acid, malic acid, tartaric acid was measured via FTIR LYZA 5000 WINE (Anton Paar, Graz, Austria).

2.4. Color characteristics

Grape skin was manually collected from 100 berries then frozen in liquid nitrogen before grinding into a powder. Then, 5 mL methyl alcohol was added to 1 g of each grape sample. Grape samples were undergoing ultrasonication for 10 min before shaking for 30 min. The samples were then extracted via centrifugation (7650 g, 5 min) twice using 5 mL methyl alcohol solution, and both supernatants were collected. Color for anthocyanin extraction liquid was measured with a spectrophotometer (CM-5, Konica Minolta, Inc., Japan). *L**(brightness-darkness), *a**(redness-greenness), *b**(yellowness-blueness), C (chromi-nance), and *h* color space data values were recorded. Values were calculated using illuminant D65 and a 10° observer. Total color differ-ences (Delta E, △E) were calculated through the following equation Akgun & Unluturk (2017).

$$\Delta E = \sqrt{\left(\Delta L^*\right)^2 + \left(\Delta a^*\right)^2 + \left(\Delta b^*\right)^2}$$

2.5. High-performance liquid chromatography (HPLC) analysis of anthocyanin

The extracts from section 2.4 were filtered (0.22 μm, Nylon, Jin Teng, China), and 10 μL was used for the HPLC analysis. Chromatographic analysis was performed using a SHIMADZU LC-20A system consisting of an autosampler, a binary pump, and a diode array detector. A Phenomenex Synergi^{TM} Hydro-RP 80A column (250 × 4.6 mm, 4 μm) was used to separate anthocyanin compounds. Elution was performed using mobile phase A (water: acetonitrile: methanoic acid = 32:4:1, v/v) and mobile phase B (water: acetonitrile: methanoic acid = 16:20:1, v/v). The results for grape anthocyanins content correspond to the average of three analyses.

2.6. Transcriptome analysis

Grape skin samples at 3 DAT were collected from UVA+ and Dark treatment for transcription analysis, and five biological replicates were performed. A total of 1 μg RNA per sample was used as input material for the RNA sample preparations. Raw sequences were transformed into clean reads after data processing. These clean reads were then mapped to the reference genome sequence (ftp://ftp.ensemblgenomes.org/pub/plants/release-25/fasta/vitis_vinifera/). Genes with an adjusted p-value < 0.05 found by DESeq2 were assigned as differentially expressed. Gene ontology (Go) enrichment analysis of the differentially expressed genes (DEGs) was implemented via the Goseq R packages based Wallenius non-central hypergeometric distribution (Young, Wakefield, Smyth, & Oshlack, 2010). We used the KOBAS software to test the statistical enrichment of DEGs in KEGG pathways (Mao, Cai, Olyarchuk, & Wei, 2005). Combine blast, iTAK and Pfam to align the gene sequences to the transcription factor database were used to obtain transcription factor information, and to identify and classify the results (Zheng et al., 2016). DEGs involved in the anthocyanin biosynthesis pathway were selected for qRT-PCR analysis (Figure S3). The process of RNA extraction was done by using Universal Plant Total RNA Isolation Kit (spin column, Bioteke Corporation, Beijing, China). cDNA synthesis was finished by EasyScript® One-Step gDNA Removal and cDNA Synthesis SuperMix (TransGen Biotech, Beijing, China). qRT-PCR was performed using 2 × SYBR Green qPCR Mixture following the manufacturer's protocol (Hlingene Corporation, Shanghai, China). Three independent biological repetitions with three technical replicates were performed.

2.7. Metabolome analysis

Grape skin and flesh samples at 3 DAT were collected from UVA+ and Dark treatment for metabolome analysis, and five biological replicates were performed. The LC/MS system for non-targeted metabolomic analysis consists of a Waters Acquity I-Class PLUS UHPLC tandem Waters Xevo G2-XS QT of the high-resolution mass spectrometer. Mobile phase A was 0.1 % formic acid, and phase B was 0.1 % formic acid and acetonitrile. The injection volume was 1 μL. The raw data files generated by Waters Xevo G2-XS QTof high-resolution mass spectrometer (MassLynx V4.2, Waters) were processed using Progenesis QI to perform peak alignment, peak picking, and quantitation for each metabolite. These metabolites were annotated using the KEGG, HMDB, and Lipidmaps databases. Principal component analysis (PCA) and partial least squares discriminant analysis (PLS-DA) was performed using BMK Cloud. Differential metabolites were chosen by value of VIP (variable importance in projection) > 1, p-value < 0.05, and fold change (FC) ≥ 2 or FC ≤ 0.5. Volcano plots were constructed on the value of $\log_2$ (FC) and $-\log_{10}$ (p-value) to filter metabolites.

2.8. Transcriptome and metabolome conjoint analysis

Weighted gene co-expression network analysis (WGCNA) was applied to obtain the gene sets with a solid correlation with flavonoid and anthocyanin biosynthesis. The expression values of 10,428 genes were obtained and used to construct the co-expression module using the WGCNA online (http://www.biocloud.net/) to perform the analysis. Parameters were set up as power = 1, MEDissThres = 0.25, and minModuleSize = 30. Differentially accumulated metabolites in the flavonoid and anthocyanin biosynthesis were simultaneously mapped to the co-expression module. Data were screened using a p value of < 0.05 to identify significant relationships. Significant associations were calculated using Pearson's correlation coefficient and were visualized using a heatmap. Hub genes were identified through cut-off values for the degree (number of neighbors) and strength (correlations in the network) and were visualized using Cytoscape v3.9.0.

2.9. Statistical analysis

All data were presented as means with the standard deviation (at least three replications). Two-way analysis of variance (ANOVA) was applied using Graphpad Prism 9.0 with Sidak's multiple comparisons test at $p < 0.05$.

3. Results

3.1. Development changes in sugar and acid components under UVA−

The CK group showed higher concentrations of glucose, fructose, and total soluble solid than the UVA− group between 2020 and 2021 (Figure S4). However, titratable acid and malic acid showed higher concentrations in the UVA− group than in the CK group. In 2020, tartaric acid consisted of titratable and malic acid, however, this was not consistently observed in the subsequent season (2021). These results showed that UVA− treatment would decline the concentration of sugar components and improve the acid components.

3.2. UVA screening changed color characteristics and decreased the anthocyanin content

The skin color indices (L^* [brightness], a^* [redness], b^* [yellowness], C^* [chroma], h [hue angle], and $\triangle E$ [total chromatic aberration]), and nine monomeric anthocyanin components of the two treatments were measured (Table 1, 2). Compared with the CK group, the UVA− group had higher levels of L^*, b^*, and C^* (except 40 and 54), and h (hue angle, except 40), indicating the elevation of skin color brightness and yellowness. In contrast, the a^* value in UVA− group was lower than that in the CK group, except for 40 DAT. $\triangle E$ values varied from 40 to 103 DAT, and the highest value appeared in the 96 DAT. To explore the possible cause of the observed inhibitory effect on grape skin color, we examined the components and contents of anthocyanin. As shown in Table 2, the content of total anthocyanin and nine monomeric anthocyanins was significantly decreased in the UVA− group compared with the CK group from 40 to 103 DAT during two seasons. Notably, four acylation anthocyanin components (Pn-3-acetylglc, Mv-3-acetylglc, Pn-3-p-coumglc, Mv-3-p-coumglc) were not detected at 40 and 54 DAT in the later year of 2021, this indicated that the effect of UVA screening was more pronounced in the early stage and concentrated on acylation anthocyanin biosynthesis.

3.3. Irradiation with UVA light promoted the color formation and improved the anthocyanin content

Additional experiments involved irradiation with UVA light (UVA+) in the incubator to demonstrate its roles in skin color formation (Table S3, S4). The samples were collected every 3 days after treatment

Table 1

Morphological and color phenotype observation of grape cluster in 6 stages.

Samples	40		54		68		82		96		103	
	CK	UVA−	CK	UVA−	CK	UVA−	CK	UVA−	CK	UVA−	CK	UVA−

Samples	40		54		68		82		96		103	
	CK	UVA−	CK	UVA−	CK	UVA−	CK	UVA−	CK	UVA−	CK	UVA−
L^*	84.28±0.23a	83.91±0.17a	84.83±0.11a	87.01±0.02b	63.27±0.01a	79.41±0.01b	68.51±0.04a	70.55±0.05b	62.99±0.02a	74.21±0.15b	61.96±0.04a	69.71±0.21b
a^*	−5.04±0.03	−3.98±0.01	−6.22±0.02	−8.26±0.05	3.32±0.05	−1.97±0.01	0.21±0.00	−2.21±0.07	4.78±0.09	−6.13±0.03	4.43±0.03	−0.93±0.01
	a	b	b	a	b	a	a	b	a	b	b	a
b^*	56.71±0.05b	47.55±0.02a	58.80±0.23b	55.72±0.12a	60.85±0.42a	61.15±0.15a	51.09±0.07a	58.46±0.07b	38.52±0.02a	56.46±0.11b	38.11±0.24a	41.81±0.23b
C^*	56.93±0.01b	47.71±0.03a	59.13±0.21b	56.33±0.17a	60.94±0.35a	61.18±0.23a	51.09±0.09a	58.51±0.22b	38.81±0.04a	56.79±0.11b	38.37±0.38a	41.82±0.17b
h	95.08±0.41a	94.79±0.37a	96.04±0.45a	98.43±0.28b	86.88±0.17a	91.84±0.29b	89.77±0.41a	92.17±0.39b	82.93±0.33a	96.20±0.05b	83.37±0.19a	91.27±0.11b
$\triangle E$	9.23±0.07		4.29±0.31		16.99±0.27		8.02±0.07		23.81±0.17		10.12±0.17	

	40 CK	40 UVA−	54 CK	54 UVA−	68 CK	68 UVA−	82 CK	82 UVA−	96 CK	96 UVA−	103 CK	103 UVA−
L^*	84.28 ± 0.23a	83.91 ± 0.17a	84.83 ± 0.11a	87.01 ± 0.02b	63.27 ± 0.01a	79.41 ± 0.01b	68.51 ± 0.04a	70.55 ± 0.05b	62.99 ± 0.02a	74.21 ± 0.15b	61.96 ± 0.04a	69.71 ± 0.21b
a^*	−5.04 ± 0.03 a	−3.98 ± 0.01 b	−6.22 ± 0.02 b	−8.26 ± 0.05 a	3.32 ± 0.05 b	−1.97 ± 0.01 a	0.21 ± 0.00 b	−2.21 ± 0.07 a	4.78 ± 0.09 b	−6.13 ± 0.03 a	4.43 ± 0.03 b	−0.93 ± 0.01 a
b^*	56.71 ± 0.05b	47.55 ± 0.02a	58.80 ± 0.23b	55.72 ± 0.12a	60.85 ± 0.42a	61.15 ± 0.15a	51.09 ± 0.07a	58.46 ± 0.07b	38.52 ± 0.02a	56.46 ± 0.11b	38.11 ± 0.24a	41.81 ± 0.23b
C^*	56.93 ± 0.01b	47.71 ± 0.03a	59.13 ± 0.21b	56.33 ± 0.17a	60.94 ± 0.35a	61.18 ± 0.23a	51.09 ± 0.09a	58.51 ± 0.22b	38.81 ± 0.04a	56.79 ± 0.11b	38.37 ± 0.38a	41.82 ± 0.17b
h	95.08 ± 0.41a	94.79 ± 0.37a	96.04 ± 0.45a	98.43 ± 0.28b	86.88 ± 0.17a	91.84 ± 0.29b	89.77 ± 0.41a	92.17 ± 0.39b	82.93 ± 0.33a	96.20 ± 0.05b	83.37 ± 0.19a	91.27 ± 0.11b
$\triangle E$	9.23 ± 0.07		4.29 ± 0.31		16.99 ± 0.27		8.02 ± 0.07		23.81 ± 0.17		10.12 ± 0.17	

Letters 'a' and 'b' indicate statistically significant differences between CK and UVA- values, as determined by a one-way analysis of variance (ANOVA) with Duncan's multiple range test ($p < 0.05$).

Table 2
Monomeric anthocyanins content under UVA− treatment in 2020 and 2021.

Year	DAT	mg/kg (FW)	Dp 3-O-Glu	Cy 3-O-Glu	Pt 3-O-Glu	Pn 3-O-Glu	Mv 3-O-Glu	Pn-3-acetylglc	Mv-3-acetylglc	Pn-3-p-coumglc	Mv-3-p-coumglc	Total anthocyanin
2020	40	CK	7.86 ± 0.33a	2.41 ± 0.15	3.36 ± 0.36	5.90 ± 0.89a	16.39 ± 0.27a	3.06 ± 0.06a	11.19 ± 0.26a	2.81 ± 0.03a	5.93 ± 0.08a	65.48 ± 1.79a
		UVA−	3.67 ± 0.03b	n.d.	n.d.	2.67 ± 0.01b	6.97 ± 0.05b	2.42 ± 0.00b	5.99 ± 0.01b	1.91 ± 0.02b	3.59 ± 0.00b	33.47 ± 1.26b
	54	CK	45.85 ± 0.08a	12.99 ± 0.02a	42.87 ± 0.11a	76.80 ± 0.35a	403.50 ± 0.74a	39.65 ± 0.07a	186.11 ± 2.43a	27.61 ± 0.17a	127.50 ± 0.24a	1198.77 ± 1.71a
		UVA−	10.91 ± 0.20b	2.68 ± 0.02b	10.41 ± 0.07b	15.72 ± 0.86b	153.73 ± 0.70b	11.22 ± 0.85b	157.34 ± 0.87b	8.65 ± 0.04b	64.71 ± 0.35b	452.26 ± 2.24b
	68	CK	25.18 ± 0.22a	7.77 ± 0.17a	25.42 ± 0.14a	64.73 ± 0.24a	296.03 ± 1.07a	30.78 ± 0.21a	245.75 ± 0.72a	15.34 ± 0.03a	72.15 ± 0.38a	837.05 ± 2.97a
		UVA−	11.28 ± 0.07b	4.18 ± 0.01b	10.72 ± 0.12b	26.12 ± 0.06b	171.23 ± 0.46b	16.72 ± 0.27b	163.91 ± 0.60b	14.38 ± 0.01b	75.89 ± 0.22b	519.46 ± 0.46b
	82	CK	47.28 ± 0.13a	8.98 ± 0.04a	53.65 ± 0.59a	108.61 ± 1.11a	764.08 ± 5.35a	75.30 ± 0.69a	728.08 ± 1.64a	39.16 ± 0.28a	219.27 ± 1.57a	2183.98 ± 6.95a
		UVA−	20.66 ± 0.46b	3.74 ± 0.01b	24.77 ± 0.15b	43.76 ± 0.08b	445.56 ± 1.28b	37.28 ± 0.12b	482.29 ± 2.00b	20.68 ± 0.11b	167.52 ± 1.06b	1307.99 ± 5.50b
	96	CK	77.86 ± 0.62a	12.67 ± 0.00a	81.58 ± 0.17a	124.39 ± 0.58a	957.57 ± 5.38a	69.72 ± 0.29a	772.26 ± 5.25a	41.35 ± 0.35a	261.73 ± 1.95a	2553.60 ± 12.64a
		UVA−	22.60 ± 0.10b	3.59 ± 0.01b	27.46 ± 0.09b	56.04 ± 1.15b	598.20 ± 11.60b	46.26 ± 1.67b	629.55 ± 1.47b	28.70 ± 0.57b	240.91 ± 0.50b	1731.55 ± 6.94b
	103	CK	66.81 ± 0.04a	12.25 ± 0.05a	68.80 ± 0.03a	122.86 ± 0.21a	864.84 ± 0.34a	67.36 ± 0.44a	698.09 ± 2.10a	42.37 ± 0.14a	260.53 ± 0.78a	2334.70 ± 0.14a
		UVA−	19.52 ± 0.12b	4.98 ± 0.01b	23.46 ± 0.15b	56.51 ± 0.54b	556.62 ± 3.43b	39.85 ± 1.41b	542.96 ± 6.69b	29.42 ± 0.14b	244.66 ± 1.90b	1575.49 ± 14.32b
2021	40	CK	2.67 ± 0.00	2.03 ± 0.37	1.77 ± 0.00	3.95 ± 0.00	11.05 ± 0.13	2.84 ± 0.09	9.35 ± 0.05	2.57 ± 0.05	4.44 ± 0.01	82.70 ± 0.53a
		UVA−	n.d.	n.d.	n.d.	n.d.	n.d.	n.d.	n.d.	n.d.	n.d.	58.72 ± 5.29b
	54	CK	4.89 ± 0.01a	2.94 ± 0.02a	5.23 ± 0.09a	9.29 ± 0.07a	40.71 ± 0.04	5.43 ± 0.16	37.44 ± 0.03	3.99 ± 0.05	11.74 ± 0.01	155.53 ± 0.68a
		UVA−	2.55 ± 0.06b	2.66 ± 0.18b	3.98 ± 0.18b	4.37 ± 0.00b	n.d.	n.d.	n.d.	n.d.	n.d.	69.42 ± 0.04b
	68	CK	28.89 ± 0.71a	9.12 ± 0.24a	46.35 ± 0.45a	92.15 ± 2.68a	662.21 ± 7.51a	50.40 ± 0.21a	564.29 ± 4.56a	22.57 ± 0.35a	135.19 ± 1.04a	1767.68 ± 17.99a
		UVA−	4.69 ± 0.01b	2.71 ± 0.01b	7.59 ± 0.45b	23.33 ± 0.28b	200.58 ± 0.55b	17.19 ± 0.00b	221.60 ± 0.69b	7.96 ± 0.01b	53.45 ± 0.16b	600.95 ± 2.14b
	82	CK	35.82 ± 1.10a	9.57 ± 0.32a	44.64 ± 0.55a	86.37 ± 0.99a	595.82 ± 5.61a	48.65 ± 0.15a	489.28 ± 4.26a	21.72 ± 0.34a	120.28 ± 0.81a	1607.59 ± 14.26a
		UVA−	8.30 ± 0.12b	3.61 ± 0.07b	12.39 ± 0.26b	35.09 ± 0.18b	265.69 ± 0.98b	24.87 ± 0.01b	258.48 ± 0.40b	11.41 ± 0.02b	66.67 ± 0.24b	760.75 ± 1.42b
	96	CK	24.21 ± 0.25a	6.97 ± 0.07a	42.02 ± 0.40a	132.73 ± 0.69a	822.54 ± 4.05a	84.09 ± 0.18a	680.20 ± 2.32a	30.09 ± 0.18a	138.82 ± 0.34a	2156.81 ± 4.62a
		UVA−	5.90 ± 0.17b	3.14 ± 0.03b	12.07 ± 0.18b	55.22 ± 0.31b	353.67 ± 2.34b	38.65 ± 0.26b	351.84 ± 2.81b	10.62 ± 0.11b	52.76 ± 0.61b	971.69 ± 4.64b
	103	CK	51.90 ± 0.10a	14.27 ± 0.05a	59.25 ± 0.17a	146.36 ± 0.02a	942.39 ± 1.85a	81.68 ± 0.22a	740.57 ± 1.51a	55.47 ± 0.29a	266.65 ± 0.48a	2561.09 ± 1.81a
		UVA−	16.14 ± 0.28b	4.33 ± 0.06b	24.46 ± 0.04b	69.62 ± 0.83b	634.38 ± 4.93b	51.42 ± 0.56b	591.93 ± 4.77b	43.05 ± 0.09b	257.49 ± 2.30b	1811.88 ± 15.04b

Delphinidin 3-O-glucoside (Dp 3-O-Glu), Cyanidin 3-O-glucoside (Cy 3-O-Glu), Petunidin 3-O-glucoside (Pt 3-O-Glu), Peonidin 3-O-glucoside (Pn 3-O-Glu), Malavidin 3-O-glucoside (Mv 3-O-Glu), Peonidin 3-O-(6-O-acetyl)-glucoside (Pn-3-acetylglc), Malavidin 3-O-(6-O-acetyl)-glucoside (Mv-3-acetylglc), Peonidin 3-O-(6-O-p-coumaryl)-glucoside (Pn-3-p-coumglc), Malavidin 3-O-(6-O-p-coumaryl)-glucoside (Mv-3-p-coumglc).
Letters 'a' and 'b' indicate statistically significant differences between CK and UVA- values, as determined by a one-way analysis of variance (ANOVA) with Duncan's multiple range test ($p < 0.05$). n.d. means not detected.

(3, 6, 9 DAT). △E showed no considerable changes from 3 to 9 DAT, and peaked value was observed in 3 DAT. Compared with the control (dark bagging), the UVA+ treatment improved a* value but decreased the values of L*(except for 3 DAT), b*, C*, h. These results contradicted those of UVA− treatment. UVA light positively promoted grape skin color formation. Similarly, UVA+ treatment increased the concentrations of total anthocyanin and that of six monomeric anthocyanins, however, this increase in concentrations was the highest on 9 DAT (Table S4). Notably, Dp 3-O-Glu and Cy 3-O-Glu were not detected under incubator conditions until 9 DAT. Pt 3-O-Glu was not detected consistently throughout the study period. Compared with the Dark group, the acylation anthocyanin contents rapidly elevated during the first two seasons in the UVA+ group. UVA radiation increased Mv-3-acetylglc concentrations to 12.60 % and 63.95 % in the control group at 6 DAT and 9 DAT, respectively. Anthocyanin levels increased significantly through UVA radiation and were suppressed through UVA screening;

thus, UVA played a positive role in anthocyanin biosynthesis. Therefore, these results confirmed that grape skins strongly responded to UVA, in particular during veraison.

3.4. Combination of screening and irradiation to analysis correlation between color characteristic and monomeric anthocyanin content

To understand the relationship between skin color and anthocyanin components, correlation analysis was performed (Figure S5). L*, b*, C*, and h were negatively correlated with anthocyanin levels, thereby indicating that an increase in anthocyanin content resulted in reduced yellowness and brightness. Conversely, a*-value was positively correlated with anthocyanin levels. Therefore, anthocyanins are typically associated with the production of the red color. Because anthocyanin levels, along with △E, rapidly increased at 3 DAT, stage 3 DAT was selected for subsequent transcriptome and metabolome analyses to

identify the candidate genes associated with UVA regulation of key anthocyanin components.

3.5. Transcriptome analyses grape skins under UVA+ treatment

A total of 3962 differentially expressed genes (DEGs) were identified at 3 DAT vs Dark comparison, which included 1995 upregulated genes and 1967 downregulated genes (Fig. 1a). Upregulated genes including *VvCHI* (VIT_01s0011g01050 and VIT_13s0067g03820), *VvDFR* (VIT_18s0001g12800), and *VvF3H* (VIT_04s0023g03370). Downregulated genes including VIT_04s0008g01160 and VIT_04s0008g00610, which belong to zf-C2H2 and zf-CCCH, respectively. Currently, all DEGs were annotated in three broad GO categories as follows: biological process, cellular component, and molecular function. The top 3 most enriched metabolism pathways were the Metabolic process, Cell, and Binding (Fig. 1b). Furthermore, 10,428 transcripts were mapped to 133 metabolic pathways through the Kyoto Encyclopedia of Genes and Genomes (KEGG). Specifically, 346, 186, and 28 transcripts were found in the phenylpropanoid biosynthesis (Ko00940), flavonoid biosynthesis pathway (Ko00941), anthocyanin biosynthesis pathway (Ko00942), respectively. The DEGs identified belonged to >19 transcription factor (TF) families; the top 5 most enriched TF families are presented with the most highly occurring member of each family

represented, including MYB, Homeobox, zf-CCCH, zf-C2H2, and ZBTB (Fig. 1c).

3.6. Metabolome analyses grape berries under UVA+ treatment

To clarify the different metabolic profiles present between the UVA+ and Dark groups, we performed orthogonal projections to latent structures-discriminant analysis (OPLS-DA). The predicted reliability of the module (Q2Y = 0.714) was effective, and the stability (R2Y = 0.996) was nearly 1, thereby indicating that the module was satisfactory (Fig. 2a). Comparing UVA+ and Dark groups revealed 136 different abundant metabolites (DAMs), consisting of 85 increased and 51 decreased metabolites. Among them, glucose content was significantly increased on UVA+ compared to Dark groups. The UVA+ and Dark groups showed remarkable changes in terms of the DAMs involved in anthocyanin synthesis and response. According to variable importance in projection (VIP) value, the top 5 DAMs were selected, and peonidin 3-(6''-acetylglucoside) [Pn-3-acetylglc] and peonidin 3-(6''-p-coumarylglucoside) [Pn-3-p-coumglc] appeared be related to anthocyanins (Fig. 2b). According to the HMDB database, DAMs can be classified as carboxylic acids and derivatives (7), fatty acyls (5), flavonoid (2), anthocyanin (1) (Fig. 2c). According to fold change, the top 20 DAMs are shown in Fig. 2d, in which malvidin 3-(6''-p-caffeyglucoside) [Mv-3-p-
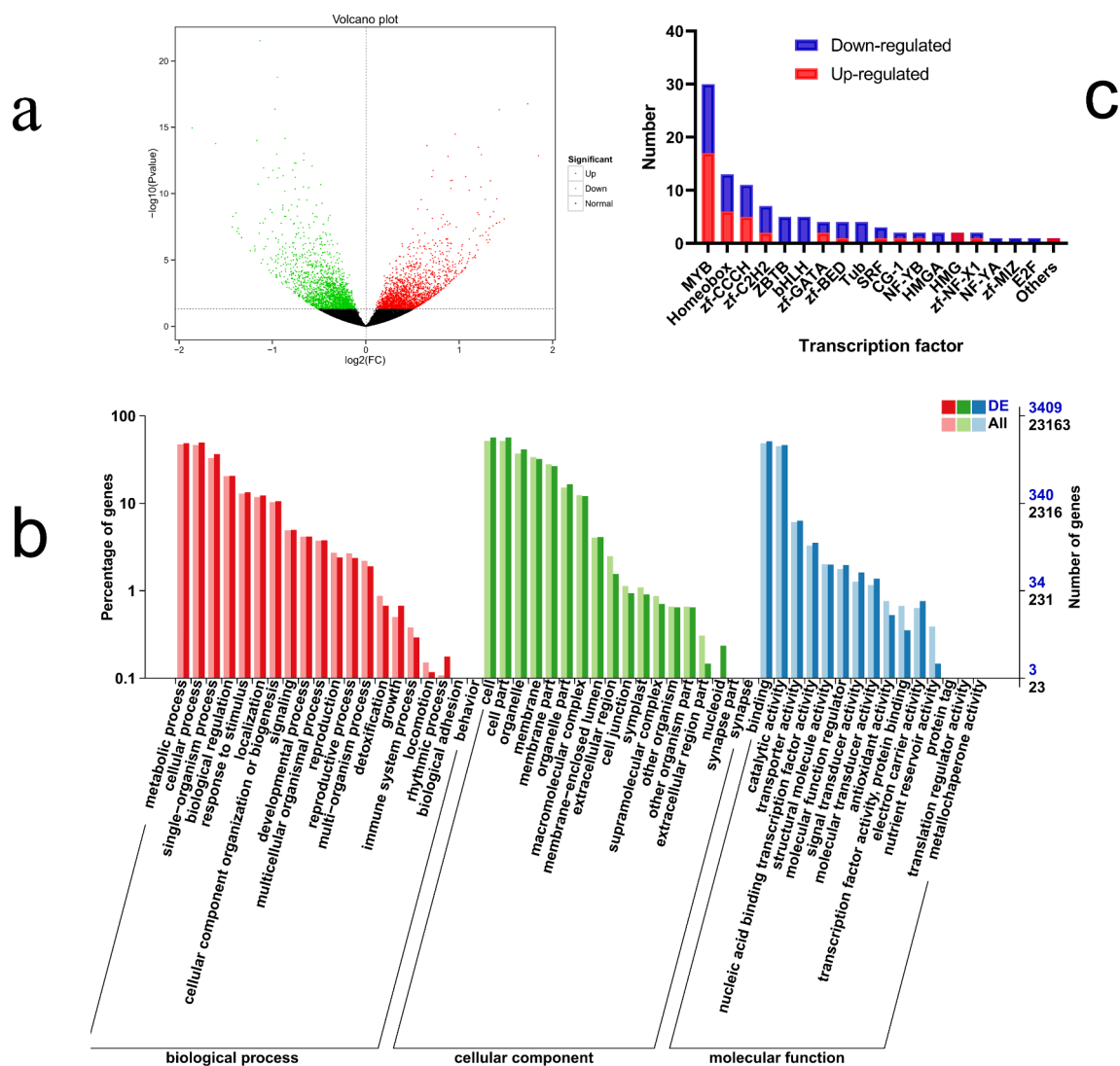

Fig. 1. Transcriptome analysis UVA irradiation (UVA+) influences berry skin during veraison. (a) Volcano plot of DEGs. (b) Go enrichment analysis of DEGs. (c) TFs prediction of DEGs.
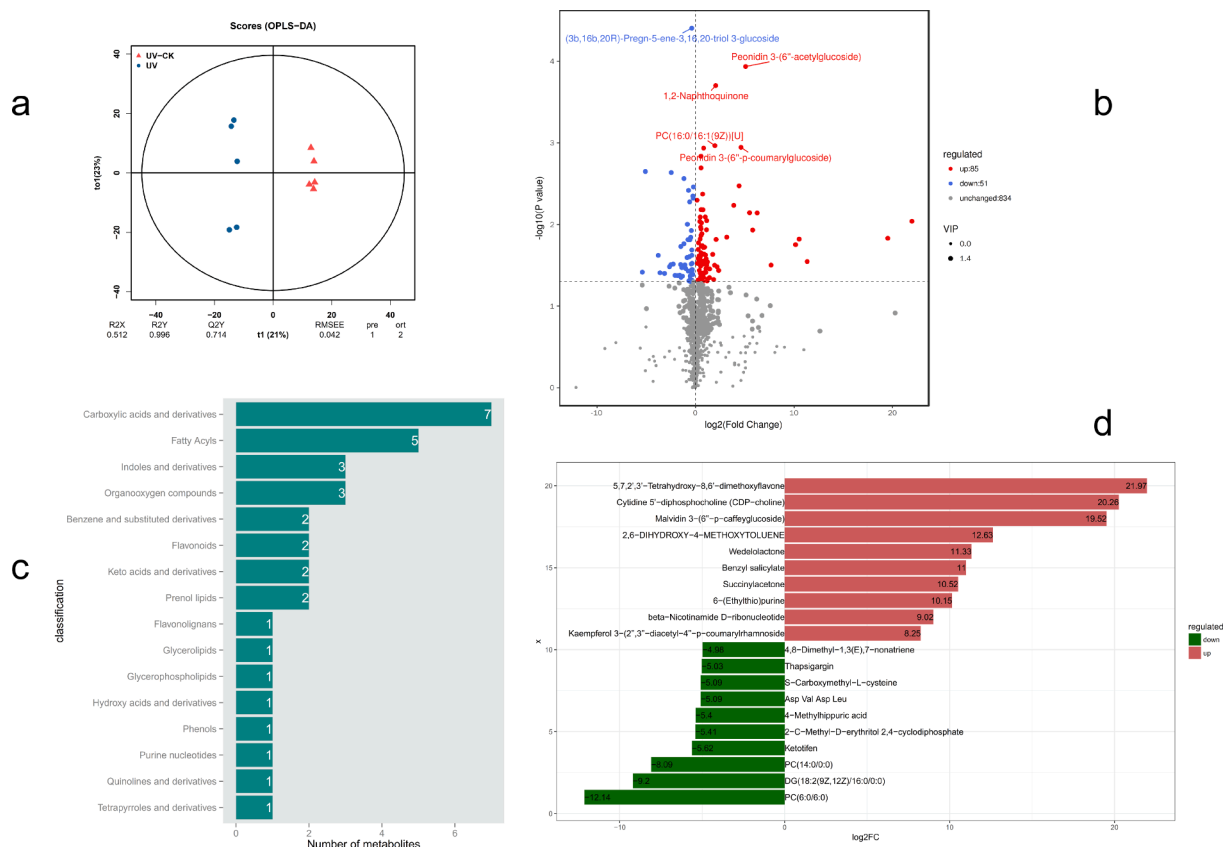
Fig. 2. Metabolome analysis UVA irradiation (UVA+) influences grape berry during veraison. (a) Scores of OPLS-DA. (b) Volcano plot of DAMs. (c) KEGG enrichment analysis of DAMs. (d) Top 20-fold change of DAMs.

caffglc] involved in anthocyanin biosynthesis improved remarkably through UVA+ treatment.

3.7. Weighted gene co-expression network analysis (WGCNA) identified the genes related to anthocyanin biosynthesis under UVA+ treatment

Genes with similar expression patterns were categorized into modules through WGCNA analysis, and 9 modules were identified in total (Fig. 3a). Modules with common expression pattern interactions in co-expression modules associated with particular traits were identified on the basis of the correlation between the module eigengene (ME) and the trait (Fig. 3b). The analysis revealed the significant association between the red module and Pn-3-acetylglc (correlation value, cor = 0.57, p-value = 0.008), Pn-3-p-coumglc (cor = 0.66, p-value = 0.002), and Apigenin 7-glucoside (cor = 0.79, p-value = 3×10^{-5}). The turquoise module was significantly associated with Mv-3-acetylglc (cor = 0.51, p-value = 0.02), Pn-3-acetylglc (cor = 0.82, p-value = 1×10^{-5}), Pn-3-p-coumglc (cor = 0.78, p-value = 4×10^{-5}), Oenin (cor = 0.51, p-value = 0.02), Apigenin 7-glucoside (cor = 0.54, p-value = 0.01), and Mv 3-O-Glu (cor = 0.54, p-value = 0.01). Functional and pathway enrichment analyses showed that the genes related to flavonoid and anthocyanin biosynthesis in the UVA+ group were concentrated in the turquoise module. Hub genes VvCHS (VIT_14s0068g00930, VIT_14s0068g00920), VIT_18s0001g09400, VvGST4 (VIT_04s0079g00690), VvPAL (VIT_13s0019g04460), VvF3′5′H (VIT_06s0009g03010, VIT_06s0009g02810, VIT_06s0009g02830, VIT_06s0009g02840), VvF3H (VIT_04s0023g03370), Vv4CL (VIT_16s0039g02040), VvCHI (VIT_13s0067g03820), had a relatively higher connectivity (Degree > 100) in the turquoise module. Additionally, three MYB TFs (VvMYBA1, VIT_02s0033g00410; VvMYB24, VIT_14s0066g01090; VIT_14s0108g00830) were identified in the turquoise module, and VvMYBA1 was played a key role in the regulatory network. Cytoscape 3.9.0 was used to construct the co-

expression network of VvMYBA1 (Fig. 3c). Further analysis showed that VvMYBA1 had a strong correlation (weight > 0.26) with VvF3H (VIT_04s0023g03370), VIT_18s0001g09400, VvANS (VIT_02s0025g04720), VvPAL (VIT_13s0019g04460), VvCHI (VIT_13s0067g03820), VvGST4 (VIT_04s0079g00690), VvF3′5′H (VIT_06s0009g03010, VIT_06s0009g02830), VvCHS (VIT_14s0068g00920, VIT_05s0136g00260, VIT_14s0068g00930), VvOMT (VIT_01s0010g03510, VIT_01s0010g03470, VIT_01s0010g03490), and VvUFGT (VIT_16s0039g02230).

3.8. Combined absence (UVA−) with abundant (UVA+) treatment to clarify the underlying mechanism of UVA controlling anthocyanin

We examined the expression of structural genes (VvCHI, VvF3′H, VvF3′5′H, VvDFR, VvLDOX, VvUFGT, and VvOMT) involved in the anthocyanin biosynthesis pathway, as well as transcriptional factor genes known to regulate anthocyanin biosynthesis (VvMYBA1, VvHY5, and VvHYH) in UVA− treatment (Fig. 4a). The expression of structural genes and TFs in the UVA− group was nearly lower than that in the control group at 40, 54, 68, and 82 DAT, this outcome was consistent with the low content of nine monomeric anthocyanins (Fig. 4a, blue box) in grape skin. Conversely, in the UVA− group, expression of the structural genes and TFs increased with maturity, and their values were higher than that in the CK group at 96 and 103 DAT, suggesting their involvement in veraison. Meanwhile, correlation analysis among relative gene expression in six stages showed that VvMYBA1 and VvHY5 were positively correlated with VvUFGT, VvHYH, and VvF3′5′H also showed a positive correlation with VvHY5 (Fig. 4b). The expression profiles of these DEGs related to anthocyanin biosynthesis are displayed in Fig. 4c. In the transcriptomic data, expression of the genes related to anthocyanin biosynthesis (VvCHS, VvCHI, VvF3′H, VvF3′5′H, VvDFR, VvLDOX, VvUFGT, and VvOMT) was higher in the UVA+ group than in the CK group (Fig. 4c). In addition, three MYB family genes VvMYBA1,
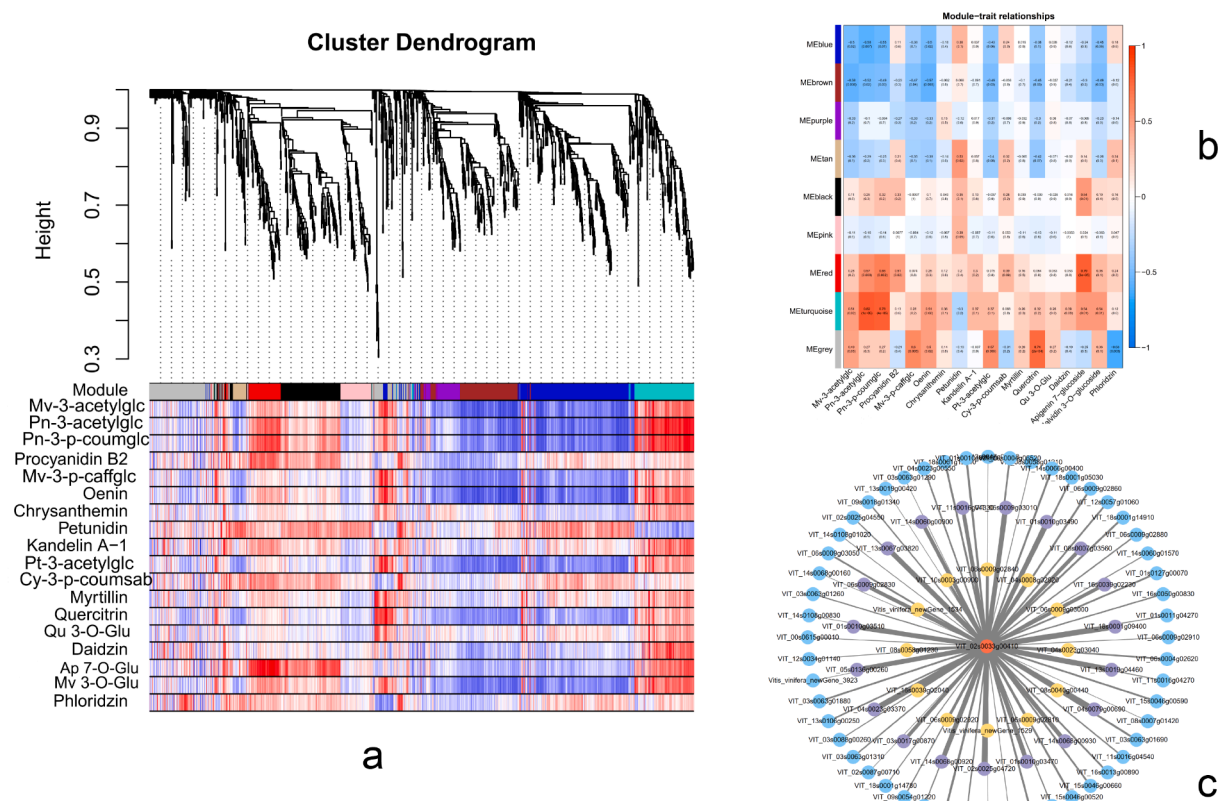
Fig. 3. Weighted gene co-expression network analysis (WGCNA) of UVA irradiation response genes in the grape skin. (a) Hierarchical cluster tree of the 31,448 common genes between different studies and the heatmap of 18 correlated metabolites enriched in flavonoid and anthocyanin biosynthesis pathway. (b) Module-trait associations. The left panel shows the 9 modules. Each cell contains the corresponding correlation and *p*-value. (c) Co-expression network analysis of the hub genes in the turquoise module. Connection strength is represented by edge width. The topological overlap measure from the WGCNA was displayed using Cytoscape to illustrate the network.

VvMYB24, and VIT_14s0108g00830, two bZIP homologues gene *VvHYH* (VIT_05s0020g01090), and *VvHY5 (VIT_04s0008g05210)*, and gene VIT_18s0001g03400 were also identified. Correlation analysis showed that *VvMYBA1* was positively correlated with *VvHYH and VvOMT*; furthermore, *VvHY5* showed a positive correlation with *VvOMT* (Fig. 4d). Meanwhile, the metabolomic analysis revealed that Pn-3-acetylglc and Pn-3-p-coumglc were the main difference in terms of the anthocyanin components in grape skin. Pn-3-acetylglc is the product of acetylglc modification, and Pn-3-p-coumglc is the product of coumaryl. Therefore, genes encoding anthocyanin acyltransferase (AAT) may tend to participate in the biosynthesis of these anthocyanins. These results showed that the UVA could modulate the co-expression of DEGs and DAMs related to phenylpropanoid metabolism, flavonoids metabolism, and biosynthesis and transport of anthocyanins during UVA irradiation.

4. Discussion

In the present study, we selected UVA+ and UVA− treatment as the research material. We characterized the floral color phenotypes and anthocyanin profiles of grape skins and performed transcriptome and metabolome analyses. Controlling network and hub genes were further identified underlying UVA radiation through WGCNA analyses.

Covering UVA screening film above grapevine reduces canopy growth and yields (Fernandes de Oliveira & Nieddu, 2016b), indicated that UVA light affects berry growth by influencing canopy physiology. UVA− treatment did reduce the concentration of anthocyanin in the skins from veraison to maturity (Table 2). Similarly, the result also demonstrated that UVA− treatment promoted a significant difference in the concentration of skin anthocyanin when compared with vines exposed to natural sunlight (Fernandes de Oliveira & Nieddu, 2016a).

The most significant responses to UVA were observed during veraison rather than harvest, however, this contradicted the result reported by Del-Castillo-Alonso et al. (2021). Excised green berries cultured in vitro underwent UVA+ treatment after dark adaptation to support this result. Anthocyanin accumulation in the berries cultured in vitro was more significant at 9 DAT after UVA+ treatment than in the berries in the control group and was increased to 37.37 %. Therefore, both UVA+ and UVA− experiments revealed that UVA light primarily contributes to anthocyanin biosynthesis in grape berries during veraison. Anthocyanins are a class of flavonoids produced during secondary metabolism and are formed by the glycosidic linkage between anthocyanidins and glycosides (Zhang et al., 2018). Glucose content was significantly decrease by UVA− and increased by UVA+ treatment. UVA− treatment respectively decreased Pn-3-acetylglc and Pn-3-p-coumglc contents to 71.70 % and 68.67 % of the control berries until 54 DAT in 2020, furthermore, monomeric anthocyanin concentrations remained at low levels from 40 to 126 DAT (Table 2). UVA+ treatment remarkably promoted Pn-3-acetylglc, Mv-3-acetylglc, Pn-3-p-coumglc and Mv-3-p-coumglc biosynthesis, and increased contents to 19.62 %, 63.95 %, 8.35 % and 47.34 % of the control group until 9 DAT, additionally, monomeric anthocyanin concentrations remained at higher levels from 3 to 9 DAT (Table S4).A decrease in acylation anthocyanin induced by UVA− was as significant as an increase induced by UVA+, indicating that acylation anthocyanin biosynthesis in berries is stimulated explicitly via UVA.

Flavones and flavonols are faint yellow or nearly colorless, and chalcones and aurones are responsible for producing deep yellows, whereas anthocyanins confer pink, red, and purple flowers, fruits, and other organs (Luo et al., 2021). In the present study, we showed that the contents of Pn 3-*O*-Glu, Mv 3-*O*-Glu, Pn-3-acetylglc, Mv-3-acetylglc, Pn-
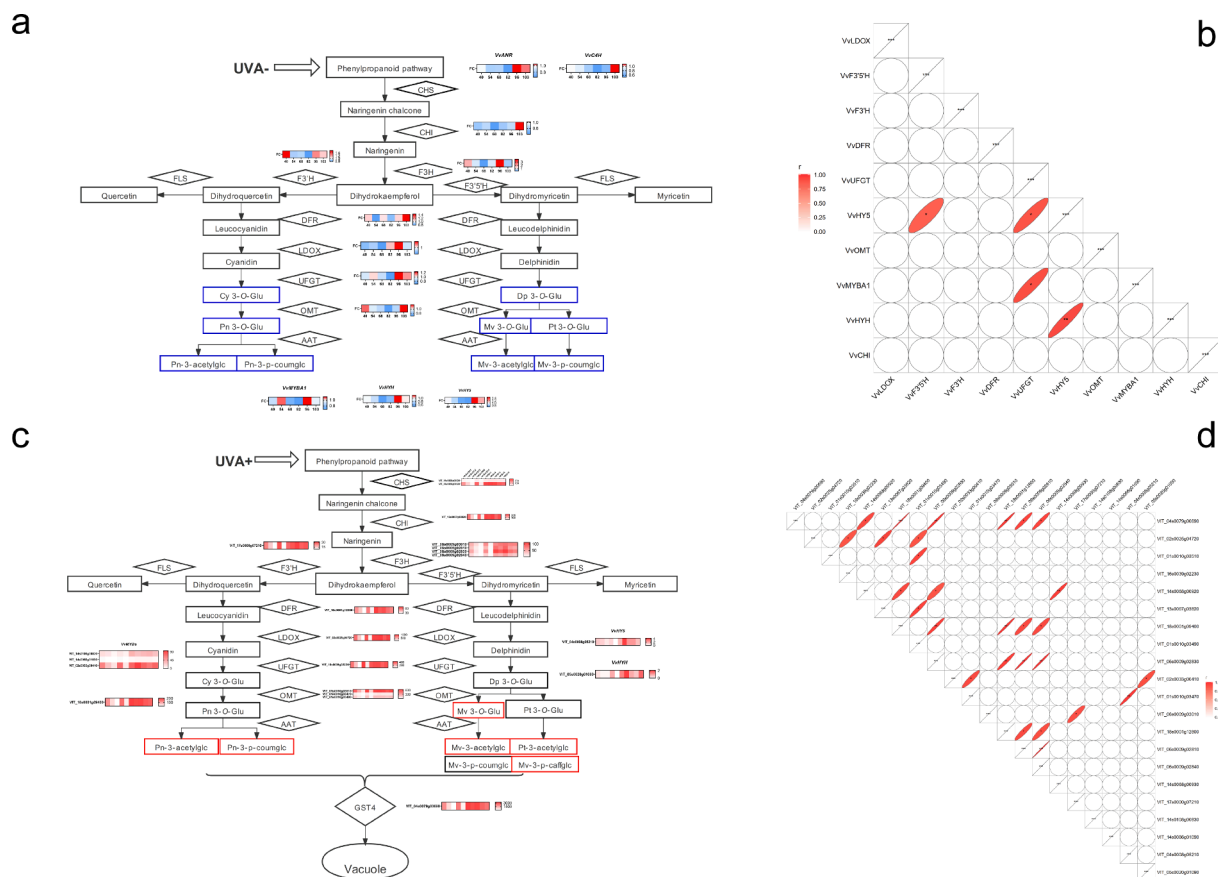
Fig. 4. Mechanism of UVA controlling anthocyanin biosynthesis. (a) Relative expression levels (fold change) of selected structural genes and transcription factor (TF) genes related in anthocyanin biosynthesis and content changes of anthocyanin components under UVA− (b) Correlations between structural genes and TF genes related in anthocyanin biosynthesis under UVA− (c) Relative expression levels (fold change) of selected structural genes and TF genes related in anthocyanin biosynthesis and relative content changes of anthocyanin components under UVA+ (d) Correlations between structural genes and TF genes related in anthocyanin biosynthesis under UVA+.

3-p-coumglc, and Mv-3-p-coumglc in the skins of UVA+ were remarkably low in the CK group. Moreover, the above monomeric anthocyanins were not detected during 3 DAT. Blueness appeared to appear more pronounced with the increase in free hydroxyl groups, whereas the intensity of the redness increased with increasing hydroxyl group methylation. The methylation anthocyanin components (Pn 3-*O*-Glu, Mv 3-*O*-Glu) we determined were increased with UVA radiation (Table S4). Furthermore, the high amount of acylation anthocyanin has been speculated to be an important reason for the color stability (He et al., 2010; Oliveira, Perez-Gregório, de Freitas, Mateus, & Fernandes, 2019). Consequently, the accumulation of the dominant anthocyanin acetylglc and coumglc is the most plausible reason for its skin color change in UVA radiation. Reductions in anthocyanin concentrations reportedly increased the *L**-value and decreased the *a**-value and resulted in changes in flower colors from red to yellow. However, the accumulation of the dominant anthocyanin Pn 3-*O*-Glu is the most likely reason for purple-red-colored in "Roufurong" petals (Guo, Wang, da Silva, Fan, & Yu, 2019; Luo et al., 2021; Sun, Yang, & Yuan, 2015). The grape's *L**-value and *a**-value were negatively and positively correlated with acetylglc and coumglc anthocyanins, respectively. The *a**-value decreased significantly with the decrease in the contents of acetylglc and coumglc anthocyanins in the UVA− group. Conversely the *a**-value increased significantly with the increase in the contents of acetylglc and coumglc anthocyanins in the UVA+ group, thereby confirming its function in the red pigmentation of grape skin.

A schematic showing significant gene expression changes related to anthocyanin biosynthesis during grape berries veraison was constructed based on the transcriptome and metabolome (Fig. 4c). The DEGs in the

UVA+ and those in the CK groups, such as *VvANR* and VvC4H, were related to phenylpropanoid biosynthesis. Except for phenylpropanoid biosynthesis, the DEGs were mainly enriched in anthocyanin biosynthesis (*VvCHS*, *VvCHI*, *VvF3'H*, *VvF3'5'H*, *VvDFR*, *VvLDOX*, *VvUFGT*, *VvOMT*, and *VvGST4*). Consequently, the DAMs of anthocyanin components were mainly enriched (Mv 3-*O*-Glu, Mv-3-acetylglc, Pt-3-acetylglc, Mv-3-p-cafflglc, Pn-3-acetylglc, and Pn-3-p-coumglc). These results showed that UVA exposure could modulate the co-expression of DEGs and DEMs related to phenylpropanoid, flavonoid, and anthocyanin biosynthesis during veraison. Further in-depth investigation of the action of the genes identified in this study may explain specific aspects of grape berries pigmentation and antioxidant properties. Several isoflavonoids and flavonoid compounds appeared to increase, such as procyanidin B2, quercitrin, daidzin, phloridzin, and myrtillin, and their increase may contribute to important antioxidant activity in grapes (García-Estévez et al., 2013; Londzin et al., 2018; Zaheer, Reddy, & Giri, 2016).

Although blue and UVA light has the same photoreceptor, blue light may increase anthocyanin accumulation by stimulating PAL and CHI activities (Cheng, Wei, & Wu, 2015), UVA light showed the difference in controlling anthocyanin. UV components can generate shifts in anthocyanin biosynthesis (Fernandes de Oliveira & Nieddu, 2016a). UVA exclusion did not influence the transcript levels of PA-related genes, whereas it dramatically decreased those of flavonol-related genes (Koyama, Ikeda, Poudel, & Goto-Yamamoto, 2012). Furthermore, cytological and biochemical analyses confirmed that the response to UVA in grape berries was independent of UVB and UVC and was correlated with the levels of anthocyanin and the expression of

structural genes and TFs. Notably, the substrate competition mechanism between FLS and DFR may lead to variation in anthocyanin and flavonol synthesis, as DFR strengthens dihydroflavonol flux toward anthocyanin and finally limits flavonol accumulation (Davies et al., 2003). Based on these results, WGCNA analysis was performed using RNA-seq data and DAMs related to flavonoid and anthocyanin biosynthesis. We noted that the turquoise module showed a considerable correlation with acetylglc- and coumglc-Pn anthocyanin. MYBs are critical TFs that regulate flavonoid biosynthesis in plants (Zhao et al., 2012), three TFs of the MYB gene family were found in this module. Consistent with this finding, the *VvMYB24* reportedly responded to UV radiation (Carbonell-Bejerano et al., 2014; Malacarne et al., 2015). Of these, *VvMYBA1* was considered a core of the controlling network (Fig. 3c). *VvMYBA1* also positively correlated with *VvHYH* and *VvOMT* (Fig. 4d). *VvHYH* was considered a part of the light-responsive TF genes (Zhang et al., 2021), implying that it might form a complex with *VvMYBA1* interaction sites to regulate downstream structural genes positively induced by UVA light. However, *VvMYBA1* is identified as a positive anthocyanin regulator (Jiu et al., 2021), *VvMYBA1* might directly regulate *VvOMT* to methylate hydroxypyrazines. Similarly, the MYB haplotype composition *trans*-regulation of the *VvF3′5′H/F3′H* expression ratio and *VvOMT* expression to affect the ratios of tri- to di-hydroxylated anthocyanins (Azuma, 2018). In the anthocyanin biosynthesis pathway, F3′H and F3′5′H catalyze the synthesis of critical intermediates, dihydroquercetin, and dihydromyricetin, respectively. These intermediates are then isomerized by DFR, LDOX, UFGT, and OMT, resulting in the production of Pn 3-*O*-Glu, Mv 3-*O*-Glu, and Pt 3-*O*-Glu. In the present study, we observed a higher expression of *VvDFR*, which may have contributed to anthocyanin biosynthesis. The OMT genotype affects the methylated/non-methylated ratio through *cis*-regulation of OMT expression (Azuma, 2018). We also observed that *VvOMT* was positively correlated with *VvHY5* (Fig. 4d). The pigment content is affected by a number of these factors, such as GST4, which is required in combination with antho-MATE, to transporter anthocyanin, thereby affecting anthocyanin content in the vacuole (Azuma, Yakushiji, Koshita, & Kobayashi, 2012; Hu et al., 2016). *VvHY5* and *VvHYH* as light signal transcription factors were upregulated via UV radiation in the berry skin (Carbonell-Bejerano et al., 2014). The high expression levels of *VvHY5*, *VvMYBA1* and *VvOMT* may promote anthocyanin production in UVA+ conditions, and low expression of these genes may inhibit anthocyanin production in UVA− conditions. Meanwhile, correlation analysis among relative gene expression from veraison to harvest showed that *VvMYBA1* and *VvHY5* were positively correlated with *VvUFGT*, *VvHYH*, and *VvF3′5′H*, however, *VvMYBA1* also showed a positive correlation with *VvHY5* (Fig. 4b). Finally, these genes that are upregulated by UVA, could be considered suitable candidate genes to elucidate their role in the regulation of acylated anthocyanins pathways.

UVA radiation can significantly enhance the contents and rates of anthocyanin accumulation and color index of "Cabernet Sauvignon" wine grape, and applications at veraison result in a higher response. Acetylation and p-coumaroylation anthocyanin were the main anthocyanin compounds involved in UVA− induced coloration. Our study showed that *VvMYBA1* might influence the accumulation of acylation anthocyanins by indirectly or directly regulating *VvOMT* expression and increasing the flux to the vacuole (through *VvGST4*), thereby ultimately contributing to the formation of red skin in grape berries during veraison. An increase in UVA radiation can improve the color formation and stability of 'Cabernet Sauvignon' wine grapes.

Declaration of Competing Interest

The authors declare that they have no known competing financial interests or personal relationships that could have appeared to influence the work reported in this paper.

Data availability

The transcriptome sequencing data are available from the NCBI under project ID PRJNA813180.

Appendix A. Supplementary data

Supplementary data to this article can be found online at https://doi.org/10.1016/j.fochms.2022.100142.

References

Akgun, M. P., & Unluturk, S. (2017). Effects of ultraviolet light emitting diodes (LEDs) on microbial and enzyme inactivation of apple. *International Journal of Food Microbiology, 260*, 65–74. https://doi.org/10.1016/j.ijfoodmicro.2017.08.007

Azuma, A. (2018). Genetic and environmental impacts on the biosynthesis of anthocyanins in grapes. *Horticulture Journal, 87*, 1–17. https://doi.org/10.2503/hortj.OKD-IR02

Azuma, A., Yakushiji, H., Koshita, Y., & Kobayashi, S. (2012). Flavonoid biosynthesis-related genes in grape skin are differentially regulated by temperature and light conditions. *Planta, 236*, 1067–1080. https://doi.org/10.1007/s00425-012-1650-x

Blancquaert, E. H., Oberholster, A., Ricardo-da-Silva, J. M., & Deloire, A. J. (2019). Effects of abiotic factors on phenolic compounds in the grape berry - a review. *South African Journal of Enology and Viticulture, 40*, 1–14. https://doi.org/10.21548/40-1-3060.

Bogs, J., Jaffé, F. W., Takos, A. M., Walker, A. R., & Robinson, S. P. (2007). The grapevine transcription factor VvMYBPA1 regulates proanthocyanidin synthesis during fruit development. *Plant Physiology, 143*, 1347–1361. https://doi.org/10.1104/pp.106.093203

Cantos, E., Espín, J. C., Fernández, M. J., Oliva, J., & Tomás-Barberán, F. A. (2003). Postharvest UV-C-irradiated grapes as a potential source for producing stilbene-enriched red wines. *Journal of Agricultural and Food Chemistry, 51*, 1208–1214. https://doi.org/10.1021/jf020939z

Cantos, E., García-Viguera, C., de Pascual-Teresa, S., & Tomás-Barberán, F. A. (2000). Effect of postharvest ultraviolet irradiation on resveratrol and other phenolics of cv. Napoleon table grapes. *Journal of Agricultural and Food Chemistry, 48*, 4606–4612. https://doi.org/10.1021/jf0002948

Carbonell-Bejerano, P., Diago, M.-P., Martínez-Abaigar, J., Martínez-Zapater, J. M., Tardáguila, J., & Núñez-Olivera, E. (2014). Solar ultraviolet radiation is necessary to enhance grapevine fruit ripening transcriptional and phenolic responses. *BMC Plant Biology, 14*, 183. https://doi.org/10.1186/1471-2229-14-183

Cheng, J. H., Wei, L. Z., & Wu, J. (2015). Effect of light quality selective plastic films on anthocyanin biosynthesis in *Vitis vinifera* L. cv. Yatomi Rosa. *Journal of Agricultural Science and Technology, 17*, 157–166. https://doi.org/10.21548/29-1-1451.

Csepregi, K., Teszlak, P., Korosi, L., & Hideg, E. (2019). Changes in grapevine leaf phenolic profiles during the day are temperature rather than irradiance driven. *Plant Physiology and Biochemistry, 137*, 169–178. https://doi.org/10.1016/j.plaphy.2019.02.012

Davies, K., Schwinn, K., Deroles, S., Manson, D., Lewis, D., Bloor, S., & Bradley, J. (2003). Enhancing anthocyanin production by altering competition for substrate between flavonol synthase and dihydroflavonol 4-reductase. *Euphytica, 131*, 259–268. https://doi.org/10.1023/A:1024018729349

de Oliveira, A. F., Mercenaro, L., Del Caro, A., Pretti, L., & Nieddu, G. (2015). Distinctive anthocyanin accumulation responses to temperature and natural UV radiation of two field-grown *Vitis vinifera* L. cultivars. *Molecules, 20*, 2061–2080. https://doi.org/10.3390/molecules20022061

Del-Castillo-Alonso, M. A., Monforte, L., Tomas-Las-Heras, R., Ranieri, A., Castagna, A., Martinez-Abaigar, J., & Nunez-Olivera, E. (2021). Secondary metabolites and related genes in *Vitis vinifera* L. cv. Tempranillo grapes as influenced by ultraviolet radiation and berry development. *Physiologia Plantarum, 173*, 709–724. https://doi.org/10.1111/ppl.13483

Fernandes de Oliveira, A., & Nieddu, G. (2016a). Accumulation and partitioning of anthocyanins in two red grape cultivars under natural and reduced UV solar radiation. *Australian Journal of Grape and Wine Research, 22*, 96–104. https://doi.org/10.1111/ajgw.12174

Fernandes de Oliveira, A., & Nieddu, G. (2016b). Vine growth and physiological performance of two red grape cultivars under natural and reduced UV solar radiation. *Australian Journal of Grape and Wine Research, 22*, 105–114. https://doi.org/10.1111/ajgw.12179

Figueiredo-Gonzalez, M., Cancho-Grande, B., & Simal-Gandara, J. (2013). Effects on colour and phenolic composition of sugar concentration processes in dried-on- or

dried-off-vine grapes and their aged or not natural sweet wines. *Trends in Food Science and Technology, 31*, 36–54. https://doi.org/10.1016/j.tifs.2013.02.004

García-Estévez, I., Gavara, R., Alcalde-Eon, C., Rivas-Gonzalo, J. C., Quideau, S., Escribano-Bailón, M. T., & Pina, F. (2013). Thermodynamic and kinetic properties of a new myrtillin-vescalagin hybrid pigment. *Journal of Agricultural and Food Chemistry, 61*, 11569–11578. https://doi.org/10.1021/jf403319u

Gollop, R., Even, S., Colova-Tsolova, V., & Perl, A. (2002). Expression of the grape dihydroflavonol reductase gene and analysis of its promoter region. *Journal of Experimental Botany, 53*, 1397–1409.

Gollop, R., Farhi, S., & Perl, A. (2001). Regulation of the leucoanthocyanidin dioxygenase gene expression in *Vitis vinifera. Plant Science, 161*, 579–588. https://doi.org/10.1016/S0168-9452(01)00445-9.

Guo, L., Wang, Y., da Silva, J. A. T., Fan, Y., & Yu, X. (2019). Transcriptome and chemical analysis reveal putative genes involved in flower color change in Paeonia 'Coral Sunset'. *Plant Physiology and Biochemistry, 138*, 130–139. https://doi.org/10.1016/j.plaphy.2019.02.025

He, F., Mu, L., Yan, G. L., Liang, N. N., Pan, Q. H., Wang, J., … Duan, C. Q. (2010). Biosynthesis of anthocyanins and their regulation in colored grapes. *Molecules, 15*, 9057–9091. https://doi.org/10.3390/molecules15129057

Hu, B., Zhao, J. T., Lai, B., Yonghua, Q., Wang, H. C., & Hu, G. B. (2016). LcGST4 is an anthocyanin-related glutathione S-transferase gene in Litchi chinensis Sonn. *Plant Cell Reports, 35*, 831–843. https://doi.org/10.1007/s00299-015-1924-4

Jiu, S., Guan, L., Leng, X., Zhang, K., Haider, M. S., Yu, X., … Fang, J. (2021). The role of VvMYBA2r and VvMYBA2w alleles of the MYBA2 locus in the regulation of anthocyanin biosynthesis for molecular breeding of grape (Vitis spp.) skin coloration. *Plant Biotechnology Journal, 19*, 1216–1239. https://doi.org/10.1111/pbi.13543

Kataoka, I., Sugiyama, A., & Beppu, K. (2003). Role of ultraviolet radiation in accumulation of anthocyanin in berries of 'Gros Colman' grapes (*Vitis vinifera* L.). *Journal of the Japanese Society for Horticultural Science, 72*, 1–6.

Kolb, C. A., Käser, M. A., Kopecký, J., Zotz, G., Riederer, M., & Pfündel, E. E. (2001). Effects of natural intensities of visible and ultraviolet radiation on epidermal ultraviolet screening and photosynthesis in grape leaves. *Plant Physiology, 127*, 863–875. https://doi.org/10.1104/pp.010373

Koyama, K., Ikeda, H., Poudel, P. R., & Goto-Yamamoto, N. (2012). Light quality affects flavonoid biosynthesis in young berries of Cabernet Sauvignon grape. *Phytochemistry, 78*, 54–64. https://doi.org/10.1016/j.phytochem.2012.02.026

Londzin, P., Siudak, S., Cegieła, U., Pytlik, M., Janas, A., Waligóra, A., & Folwarczna, J. (2018). Phloridzin, an apple polyphenol, exerted unfavorable effects on bone and muscle in an experimental model of type 2 diabetes in rats. *Nutrients, 10*, 1701. https://doi.org/10.3390/nu10111701

Luo, X. N., Sun, D. Y., Wang, S., Luo, S., Fu, Y. Q., Niu, L. X., … Zhang, Y. L. (2021). Integrating full-length transcriptomics and metabolomics reveals the regulatory mechanisms underlying yellow pigmentation in tree peony (Paeonia suffruticosa Andr.) flowers. *Horticulture Research, 8*, 235. https://doi.org/10.1038/s41438-021-00666-0

Malacarne, G., Costantini, L., Coller, E., Battilana, J., Velasco, R., Vrhovsek, U., … Moser, C. (2015). Regulation of flavonol content and composition in (Syrah×Pinot Noir) mature grapes: Integration of transcriptional profiling and metabolic quantitative trait locus analyses. *Journal of Experimental Botany, 66*, 4441–4453. https://doi.org/10.1093/jxb/erv243

Mao, X., Cai, T., Olyarchuk, J. G., & Wei, L. (2005). Automated genome annotation and pathway identification using the KEGG Orthology (KO) as a controlled vocabulary. *Bioinformatics, 21*, 3787–3793. https://doi.org/10.1093/bioinformatics/bti430

Oliveira, H., Perez-Gregório, R., de Freitas, V., Mateus, N., & Fernandes, I. (2019). Comparison of the in vitro gastrointestinal bioavailability of acylated and non-acylated anthocyanins: Purple-fleshed sweet potato vs red wine. *Food Chemistry, 276*, 410–418. https://doi.org/10.1016/j.foodchem.2018.09.159.

Pfuendel, E. E. (2003). Action of UV and visible radiation on chlorophyll fluorescence from dark-adapted grape leaves (*Vitis vinifera* L.). *Photosynthesis Research, 75*, 29–39.

Pfuendel, E. E., Ben Ghozlen, N., Meyer, S., & Cerovic, Z. G. (2007). Investigating UV screening in leaves by two different types of portable UV fluorimeters reveals in vivo screening by anthocyanins and carotenoids. *Photosynthesis Research, 93*, 205–221. https://doi.org/10.1007/s11120-007-9135-7

Sun, X. B., Yang, Q., & Yuan, T. (2015). Preliminary studies on the changes of flower color during the flowering period in two tree peony cultivars. *Acta Horticulturae Sinica, 42*, 930–938. https://doi.org/10.16420/j.issn.0513-353x.2014-0996.

Young, M. D., Wakefield, M. J., Smyth, G. K., & Oshlack, A. (2010). Gene ontology analysis for RNA-seq: Accounting for selection bias. *Genome Biol, 11*, R14. https://doi.org/10.1186/gb-2010-11-2-r14

Zaheer, M., Reddy, V. D., & Giri, C. C. (2016). Enhanced daidzin production from jasmonic and acetyl salicylic acid elicited hairy root cultures of *Psoralea corylifolia* L. (Fabaceae). *Natural Product Research, 30*, 1542–1547. https://doi.org/10.1080/14786419.2015.1054823

Zhang, K. K., Liu, Z. J., Guan, L., Zheng, T., Jiu, S. T., Zhu, X. D., … Fang, J. G. (2018). Changes of anthocyanin component biosynthesis in 'summer black' grape berries after the red flesh mutation occurred. *Journal of Agricultural and Food Chemistry, 66*, 9209–9218. https://doi.org/10.1021/acs.jafc.8b02150

Zhang, P. A., Lu, S. W., Liu, Z. J., Zheng, T., Dong, T. Y., Jin, H. C., … Fang, J. G. (2021). Transcriptomic and metabolomic profiling reveals the effect of LED light quality on fruit ripening and anthocyanin accumulation in Cabernet Sauvignon grape. *Frontiers in Nutrition, 8*, Article 790697. https://doi.org/10.3389/fnut.2021.790697

Zhang, Z. Z., Li, X. X., Chu, Y. N., Zhang, M. X., Wen, Y. Q., Duan, C. Q., & Pan, Q. H. (2012). Three types of ultraviolet irradiation differentially promote expression of shikimate pathway genes and production of anthocyanins in grape berries. *Plant Physiology and Biochemistry, 57*, 74–83. https://doi.org/10.1016/j.plaphy.2012.05.005

Zhao, L., Gao, L. P., Wang, H. X., Chen, X. T., Wang, Y. S., Yang, H., … Xia, T. (2012). The R2R3-MYB, bHLH, WD40, and related transcription factors in flavonoid biosynthesis. *Functional and Integrative Genomics, 13*, 75–98. https://doi.org/10.1007/s10142-012-0301-4

Zheng, Y., Jiao, C., Sun, H., Rosli, H. G., Pombo, M. A., Zhang, P., … Fei, Z. (2016). iTAK: A program for genome-wide prediction and classification of plant transcription factors, transcriptional regulators, and protein kinases. *Molecular Plant, 9*, 1667–1670. https://doi.org/10.1016/j.molp.2016.09.014